Taylor & Francis
Taylor & Francis Group

RESEARCH ARTICLE

Check for updates

A GIS-based fire spread simulator integrating a simplified physical wildland fire model and a wind field model

D. Prieto Herráez [a], M. I. Asensio Sevilla [a,b], L. Ferragut Canals [a,b],
J. M. Cascón Barbero [b,c] and A. Morillo Rodríguez [d]

aApplied Mathematics Department, University of Salamanca, Salamanca, Spain; bFundamental Physics and Mathematics University Institute, University of Salamanca, Salamanca, Spain; cEconomy and Economic History Department, University of Salamanca, Edificio FES, Campus Miguel de Unamuno, Salamanca, Spain; dSEAGA, Xunta de Galicia, Polígono Industrial do Tambre, Santiago de Compostela, Spain

ABSTRACT

This article discusses the integration of two models, namely, the Physical Forest Fire Spread (PhFFS) and the High Definition Wind Model (HDWM), into a Geographical Information System-based interface. The resulting tool automates data acquisition, preprocesses spatial data, launches the aforementioned models and displays the corresponding results in a unique environment. Our implementation uses the Python language and Esri's ArcPy library to extend the functionality of ArcMap 10.4. The PhFFS is a simplified 2D physical wildland fire spread model based on conservation equations, with convection and radiation as heat transfer mechanisms. It also includes some 3D effects. The HDWM arises from an asymptotic approximation of the Navier–Stokes equations, and provides a 3D wind velocity field in an air layer above the terrain surface. Both models can be run in standalone or coupled mode. Finally, the simulation of a real fire in Galicia (Spain) confirms that the tool developed is efficient and fully operational.

1. Introduction

According to the last available fire management global assessment from FAO (2007), the global estimate of land area affected by fire in 2000 was 350 million hectares, much of which was forest and woodland. Most of the area burned was in sub-Saharan Africa, followed at some distance by Australia. In more recent regional reports, wildfire event data can be found, some of them as devastating as in Greece in August 2007, in all the Mediterranean countries in August 2009, in European Russia during the hot summer of 2010, in boreal forest of Alberta, Canada, in 2011 and again in 2016, and the most recent in Chile in January 2017. The intensity, frequency and duration of wildland fires are now considered to be directly influenced by global warming. Wildland fires are not only a result of a changing climate; however, they also emit greenhouse gases and therefore

---

also contribute to global warming (Flannigan *et al*. 2009). Besides the huge environmental damage, wildland fires do not only bring about huge economical losses, they also cause human casualties. In brief, wildland fires have become one of the most pressing environmental, social and economical issues threatening the world's forests.

Therefore, the real-time simulation of wildland fire spread has direct applications in prevention (risk mapping, reforestation policies and the design of fuelbreaks), in firefighting (predicting a fire's pathway helps to mobilize and optimize resources, improve firefighters' safety during extinguishing works, issue warnings and evacuation planning), and in prescribed burn planning.

Numerous wildfire models have already been developed, and they can be classified into different types according to the nature of their construction: physical, semi-physical or empirical (Pastor *et al*. 2003, Sullivan 2009a, 2009b), although the nomenclature varies. Some authors argue that for a model to be classified as physical it must cater for both the physics and chemistry of the fire spread; semi-physical models are defined as those that seek to represent only the physics of the problem; and empirical models are those based on a phenomenological description or statistical regression of observed fire behaviour. According to the physical process modelled, wildland fire models can also be grouped as ground fires, surface fires, crown fires and spotting models (Pastor *et al*. 2003). Since surface fires are the most predominant, there exists an intensive research in this type of models.

The wildland fire model we propose is called Physical Forest Fire Spread (PhFFS) (Asensio and Ferragut 2002, Ferragut *et al*. 2007a, 2007b). It is a simplified 2D one-phase semi-physical model for surface fires based on the fundamental physics of combustion and fire spread, together with certain appropriate assumptions. The model considers two important forms of heat transfer in these kinds of fires, namely convection and radiation (Anderson 1969), although their relative importance varies from fire to fire, and estimating their exact combination is not simple (Frankman *et al*. 2013, Finney *et al*. 2015). The model also takes into account the heat lost by natural convection, the effect of the flame tilt by wind or slope over the heat transfer and the influence of fuel moisture content and fuel type. The numerical solution of the model equations involves efficient numerical and computational tools for simulating a real scenario in less than real time.

One of the factors most influencing wildland fire spread is the wind (Viegas 2004). The PhFFS model can use meteorological wind data or be coupled with the High Definition Wind Model (HDWM) (Asensio *et al*. 2005, Ferragut *et al*. 2011). This wind model arises from an asymptotic approximation of the Navier–Stokes equations, providing a 3D velocity wind field. It only requires meteorological wind measures at a small number of points in the simulation area, as well as information on surface topography and roughness.

Wildland fire simulation requires coupling spatial data with the simulation model. This approach calls for a spatial data management system to handle the diverse resources of information needed as input data for the wildland fire model, and for displaying the simulation results. The combination of environmental models and their spatial and temporal information using Geographical Information Systems (GISs) has been largely studied and applied (Skidmore 2002), as GIS allows building integrated database systems. Due to the spatial nature of the fire spread, GISs are widely used in wildland fire

studies (Ager *et al.* 2011). The development of wildland fire risk maps with GIS (Chuvieco and Duarte 1996) is an example of one such application. The simulation of wildland fire spread is another important and common GIS application (Yassemi *et al.* 2008, Mandel *et al.* 2014, Williams *et al.* 2014). Currently, several wildland fire spread models integrated in GIS are already being used, most of them are empirical mainly based on perimeter propagation. These models are very fast, but have many limitations, as they depend on a fire front spread rate that is generally empirically computed, in most cases by applying Rothermel's model (1972), so they are only applicable to situations in which the conditions are identical to those used in their formulation and adjustment. There are different types of perimeter propagation models: front-tracking methods, cellular methods and, more recently, level set methods (Hilton *et al.* 2015). An example of a wildfire growth model based upon front-tracking methods is FARSITE (Finney 2004), widely used in the US by federal and state land management agencies, based upon BEHAVE (Andrews 1986) fire behaviour prediction, which itself is an implementation of Rothermel's model, and produces outputs compatible with GIS software for later analysis and displays. Other examples are as follows: Prometheus (Tymstra *et al.* 2010), the Canadian Wildland Fire Growth Simulation Model, which exports simulated data for GISs; and SiroFire (Coleman and Sullivan 1996), the CSIRO Bushfire Spread Simulator developed for operational use in Australia that uses GIS-derived geographic maps and digital terrain models to graphically present the spread of the simulated fires. The models based upon cellular methods include FireStation (Lopes *et al.* 2002), which optionally imports the input data from GIS common formats, FIREMAP (Vasconcelos and Guertin 1992), which integrates the BEHAVE system and GIS using discrete event system specifications DEVS; and many others (Perry *et al.* 1999, Yassemi *et al.* 2008) also based on Rothermel's model. The more recent level-set method is the perimeter-growth approach used in the WRF-Fire model (Mandel *et al.* 2011), which couples the WRF atmosphere model and SFIRE fire spread model, again based on Rothermel's model, that has been recently integrated into a GIS (Mandel *et al.* 2014).

By contrast, physical or semi-physical models have not been so widely integrated into GIS tools due to their complexity and computational cost. One of the foremost physical wildland fire models is HIGRAD-FIRETEC (Linn *et al.* 2002), a physics-based, 3D computer code designed to simulate the interactive relationship between fire, fuels, atmosphere and topography, based on the FIRETEC fire model (Linn 1997) and the HIGRAD (Reisner *et al.* 1997) fluid-dynamics model. FIRETEC has a high computational cost, so it is presently a research tool only.

The novelty of this current work is that the wildland fire spread model integrated into GIS is a simplified physical model for faster-than-real-time simulation that also includes its own wind velocity model. Both models can be compiled for any platform, and can operate either together or separately: the PhFFS model can operate with constant wind or with wind data provided by the HDWM or any other wind model. Furthermore, the HDWM model can provide wind field data from punctual meteorological data for other purposes. The scope of application of the GIS interface developed for these two models is initially Spain, but it can be extended to other countries by compiling the corresponding maps. Both models, PhFFS and HDWM, and their integration into the commercial suite ArcGIS Desktop 10.4 tool have been developed by the same research group, providing full control of the end product.

The functionalities of Esri's software have been extended by an add-in to provide a flexible and user-friendly end-user interface for simulating a real fire and/or a wind field. This add-in permits the user to perform the preprocessing task in order to provide all the necessary data for the simulation. It also automates the input of temporal data, such as weather conditions, ignition points or fire suppression tactics. In addition, our add-in can be used to launch the simulation and, finally, to load the results for their analysis and display on a base map that is easily understood by non-specialist users. Furthermore, the accurate adjustment of both PhFFS and HDWM is one of the current challenge of their development, and their GIS integration will enable this task to be handled more easily and improve the adjustment process.

This paper is organized as follows: Section 2 reviews the physical models integrated into GIS software. Section 3 addresses the main issues in the process of developing the add-in for the ArcGIS software. Section 4 evaluates the resulting tool's performance by simulating a wildfire that occurred near Ourense (Spain) in September 2009, comparing the simulation results with the real fire's progress. Finally, the paper ends with its conclusions in Section 5.

2. The physical models

This section briefly describes the underpinnings of the two models coupled with the GIS to provide the operational wildland fire simulation GIS-based tool: PhFFS and HDWM. Both models have been developed by the research group to which most of the authors belong, the Research Group of Numerical Simulation and Scientific Calculus of the University of Salamanca. We also outline both models input and output variables and parameters as a step towards their integration into a GIS.

2.1. *Physical Forest Fire Spread*

The PhFFS is the current version in a series of physical fire propagation models. It has its origin in a simple 2D one-phase physical model, based on the principles of energy and mass conservation, and considered convection and diffusion. In due course, heat transfer by radiation was incorporated into the model with a local radiation term (Asensio and Ferragut 2002). The influences of fuel moisture content and heat absorption by pyrolysis were included by Ferragut *et al.* (2007b) with an operator representing enthalpy. At the same time, the non-local radiation from the flames above the vegetal layer was added to the model (Ferragut *et al.* 2007a), enabling it to deal with the effect that wind and slope had over flame tilt and thus increasing heat transfer. Fresh efforts have been made to improve the suitability of the PhFFS model for the simulation of real fires in Ferragut *et al.* (2014) and experimental fires in Prieto *et al.* (2015), with the introduction of data assimilation techniques in Ferragut *et al.* (2015).

The partial differential equations describing the PhFFS model are based on the energy and mass conservation equation on the surface where the fire takes place, and the radiation equation on the air layer over this surface. The model equations are not described here because of their mathematical complexity. A detailed explanation of the current PhFFS model equations can be found in Prieto *et al.* (2015), although here we briefly describe the physical meaning of each of the equations terms. We also outline the

equations unknowns, its input variables and its three parameters, that are summarized in Section 2.4, in order to understand how the PhFFS model is coupled with GIS.

The surface where the fire develops is given by a function h representing the topography; that is, the function h gives the land surface height.

The physical quantities involved as the unknowns in the model equations are enthalpy E (J m^{-2}), solid fuel temperature T (K) and fuel load M (kg m^{-2}). The following input variables are also required: the heat capacity of the solid fuel C (J K^{-1} kg^{-1}), the maximum solid fuel load M_0 (kg m^{-2}), both depending on fuel type, and the reference temperature, which is the ambient temperature T_∞ (K).

The influence of the vegetation's moisture content is modelled through an operator depending on enthalpy, the latent heat of evaporation Λ_v (J kg^{-1}), and fuel moisture content M_v (kg of water/kg of dry fuel).

The model also takes into account the energy lost by natural free convection through a term in the energy conservation equation. This term is related to the natural convection coefficient H (J s^{-1} m^{-2} K^{-1}), the first of the three model parameters.

Our model considers wind effect in two different ways: through the convective term itself and through the flame tilt caused by wind that affects the radiation term. The energy conservation equation incorporates a term representing convective heat. This term depends on the surface wind velocity, **V** (m s^{-1}), rescaled by a correction factor β, which is the second model parameter. To deeply understand the meaning of this parameter β, see Prieto et al. (2015), where it is explained how this one solid phase model is simplified from a two phase solid–gas model, and how the assumptions of this simplification allow to estimate this parameter. Surface wind velocity **V** is provided by meteorological sources. The HDWM (or any other wind model) is used to compute a 3D wind velocity field from these meteorological data. Then, the wind velocity at flame average weight is supplied as input data to PhFFS. Alternatively, surface wind velocity **V** can be considered as constant wind along the simulation area.

The thermal radiation reaching the surface from the flame is included in the energy conservation equation, taking into account the influence of wind and slope over flame tilt. The radiation equation contains the third and final model parameter, the radiation absorption coefficient a (m^{-1}), and two model variables, flame temperature denoted by T_f (K) and flame length F (m), with both depending on fuel type. For further details about radiation computation, see Ferragut et al. (2015).

An important simplification of the PhFFS model is that only the solid phase of the combustion process is considered: the solid fuel mass M varies between 0 and its maximum value M_0, and the maximum value of solid fuel temperature T is the pyrolysis temperature T_p (K). The gaseous phase is parameterized in the radiation term through flame temperature T_f, and flame length F.

The loss rate of solid fuel due to combustion is represented in the mass conservation equation. It is null when the pyrolysis temperature has not been reached, and constant once it has been exceeded. This constant value is inversely proportional to the solid fuel half-life of the combustion, $t_{1/2}$ (s), of each type of fuel, measured from the moment of ignition.

The numerical solution of the model is obtained by solving the corresponding non-dimensional partial differential equations depending on the non-dimensional

solid fuel temperature $u = \frac{T-T_\infty}{T_\infty}$, and the non-dimensional solid fuel mass fraction $c = \frac{M}{M_0}$. The numerical methods used are the finite element method combined with various finite difference schemes in time, the characteristic method for the convective term and an exact integration method assuming a rectangular flame shape section (under windy conditions we assume tilted flames) for the non-local radiation equation. With a view to reducing the computational cost of the 3D radiation equation, active nodes are defined for solving this equation only where necessary in the vicinity of the flames. These efficient numerical methods, together with different parallel computing techniques, ensure that the computational cost of running the PhFFS model has been significantly reduced, whereby it can compete with other simpler models.

The PhFFS model is implemented in C++, using API OpenMP (Chapman *et al.* 2008) in order to exploit today's multiprocessor platforms for reducing computational time. This implementation is entered in the Spanish Registry of Intellectual Property on 16 July 2015 under record entry 00/2015/4720.

2.2. *High Definition Wind Model*

The origin of the HDWM lies in an asymptotic approximation of the primitive Navier–Stokes equations considering that the horizontal dimensions are much larger than the vertical ones. The aim is to provide a 3D wind velocity field in the air layer over the surface of study, solving only 2D linear equations so that it can be coupled with the 2D fire spread model. This idea was first published in Asensio *et al.* (2002), where the coupling of wind and fire models had already been considered. The details of how this model stems from an asymptotic approximation of the Navier–Stokes equations can be found in Asensio *et al.* (2005). Roughly speaking, the HDWM locally provides a detailed 3D wind velocity field in an air layer over the surface, above which the surface temperature and topography have not effect, solving only 2D equations depending on the temperature on the ground surface T (or T_∞ in the absence of fire), topography h, and the horizontal component of the meteorological wind $v_m \cdot n$ on the boundary of the simulation air layer. The model depends on a single parameter, the friction coefficient ζ, which is related to the surface roughness length z_0 (m) using the Davenport classification of terrain (Davenport *et al.* 2000). The model takes into account slope effects, mass conservation and buoyancy forces that enable the effect of wind temperature to be included. In Ferragut *et al.* (2011), the wind velocity field obtained by the model is adjusted to several wind velocity measurements v_m at different points in the 3D domain. This adjustment requires solving an optimal control problem in which the wind flow on the surface boundary is the control. Our wind field model does not therefore require measuring the meteorological wind on the boundary, as it suffices to provide the meteorological wind at certain points in the domain, for example, the data from weather stations. Our model is an alternative for wind resource estimation in local terrains using mesoscale–microscale coupling techniques (Gopalan *et al.* 2014).

The HDWM equations are not shown in this paper due to their mathematical complexity. Interested readers can find the details in the aforementioned papers. The

implementation of the HDWM is entered in the Spanish Registry of Intellectual Property on 16 July 2015 under record entry 00/2015/4721.

2.3. Coupling PhFFS-HDWM

Coupling both HDWM and PhFFS models reveals the influence that thermal effects, such as the high temperatures that occur during a fire, have on the wind, and the effect of wind (and also slope) on the flame tilt in order to compute the radiation and thus on fire spread. The wind's effect on the fire model gauged through the convective term and the flame tilt in the radiation term is computed in a very competitive time. In general terms, the 1-h simulation of a medium size fire by the PhFFS model, updating wind data every half hour by the HDWM, is at least 10 times faster than the actual period simulated. Considering that the fire's thermal effects on wind involve updating wind data each time step on fire simulation, significantly increasing final computational time. In order to reduce this time, improvements in the code parallelization are being studied, as well as the introduction of reduced basis methods for the HDWM (Cascón et al. 2016). We do not present coupled simulation results in this paper.

2.4. Input variables, parameters and output variables

Since the aim of this work is to develop a tool that allows non-specialized users to simulate real fires in a user-friendly environment, it is important to identify the model input and output data, as a first step for integrating the PhFFS and HDWM into the final GIS tool. Figure 1 summarizes the inputs and outputs of both models, as described in this section.

Regarding the input data, we have distinguished between the input variables and the model parameters. The input variables are those magnitudes that can be measured more or less accurately, which together define a specific scenario for the modelling and
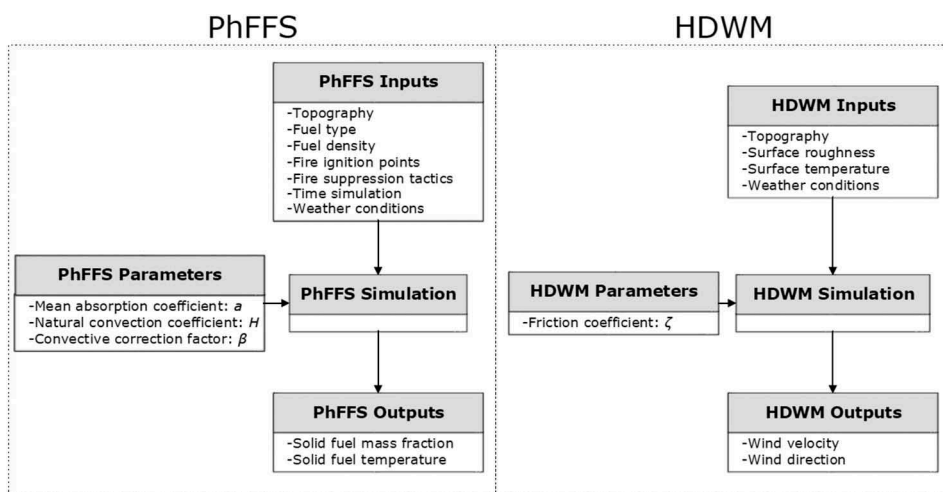

Figure 1. PhFFS and HDWM input and output data.

Table 1. PhFFS quantities, input variables and parameters.

Model quantities	Symbol	Units
Enthalpy	E	J m^{-2}
Solid fuel temperature	T	K
Fuel load	M	kg m^{-2}
Model input variables	**Symbol**	**Units**
No fuel type dependent		
Wind velocity	V	m s^{-1}
Reference temperature	T_∞	K
Surface height	h	m
Latent evaporation heat	Λ_v	J kg^{-1}
Fuel type dependent		
Maximum fuel load	M_0	kg m^{-2}
Moisture content	M_v	kg of water/kg of dry fuel
Flame temperature	T_f	K
Pyrolysis temperature	T_p	K
Combustion half-life	$t_{1/2}$	s
Flame length	F	m
Heat capacity	C	JK^{-1}kg^{-1}
Model parameters	**Symbol**	**Units**
Mean absorption coefficient	a	m^{-1}
Natural convection coefficient	H	J s^{-1}m^{-2}K^{-1}
Correction factor of convective term	β	–

the user should provide. Model parameters are unknown values, although their physical meaning can offer an approximate idea of their ranges, which should be previously adjusted. Tables 1 and 2 summarize the parameters and the input variables (fuel type and no fuel type dependent) for PhFFS and HDWM, respectively.

The necessary meteorological data, ambient temperature T_∞ and wind velocity v_m, are provided by weather stations placed in or very close to the study areas. All the other input variables, such as the height of the surface h or the fuel load M, are spatial data, and must therefore be provided via GIS.

Among the spatial data needed for HDWM and PhFFS, it is important to mention fuel type, as most of the input variables depend on fuel type. It is currently considering the BEHAVE fuel classification system (Anderson 1982), but it may be used the more recent Scott and Burgan dynamic fuel models (Scott and Burgan 2005), or even monitored data whenever available. These data are obtained from land cover or

Table 2. HDWM quantities, input variables and parameters.

Model quantities	Symbol	Units
Wind velocity	V	m s^{-1}
Potential	p	s^{-1}
Model input variables	**Symbol**	**Units**
No fuel type dependent		
Horizontal component of meteorological wind	v_m	m s^{-1}
Surface air temperature	T	K
Height of the surface	h	m
Fuel type dependent		
Roughness length	z_0	m
Model parameters	**Symbol**	**Units**
Friction coefficient	ζ	–

forestry maps, and are used as an index to establish the model input variables dependent on them.

In addition, the PhFFS model needs two more spatial input variables related to the initial conditions in the study area. One is the initial solid fuel temperature, T at time $t = 0$, which contains the information related to the ignition location. The other one is the initial fuel load, M at time $t = 0$, supplied by land cover maps that provide those points on the surface where combustibles spread the fire and those where there is no fuel, such as highways, rivers and lakes, etc.

We should recall that the corresponding non-dimensional initial solid fuel temperature $u = \frac{T-T_\infty}{T_\infty}$ and non-dimensional initial fuel load $c = \frac{M}{M_0}$ are the unknowns of the PhFFS model. At each time step, the PhFFS model provides these two spatial output variables, u and c, which will be displayed in the GIS tool.

3. Development of the GIS-based interface

This section describes all the details of the GIS interface development for the PhFFS and HDWM, as outlined in Figure 2. This interface is implemented as a *Python add-in* for the ArcMap 10.4 application of Esri's ArcGIS Desktop suite.[1] We cover all the topics related to the automation of spatial data processing and user interface development. We then discuss the geographical resources used to provide the input data the models need, and finally, we also explain how the results obtained are displayed.

3.1. *User interface*

The integration of GIS and spatio-temporal models has been widely studied, and many different approaches have been considered. These strategies can be categorized as
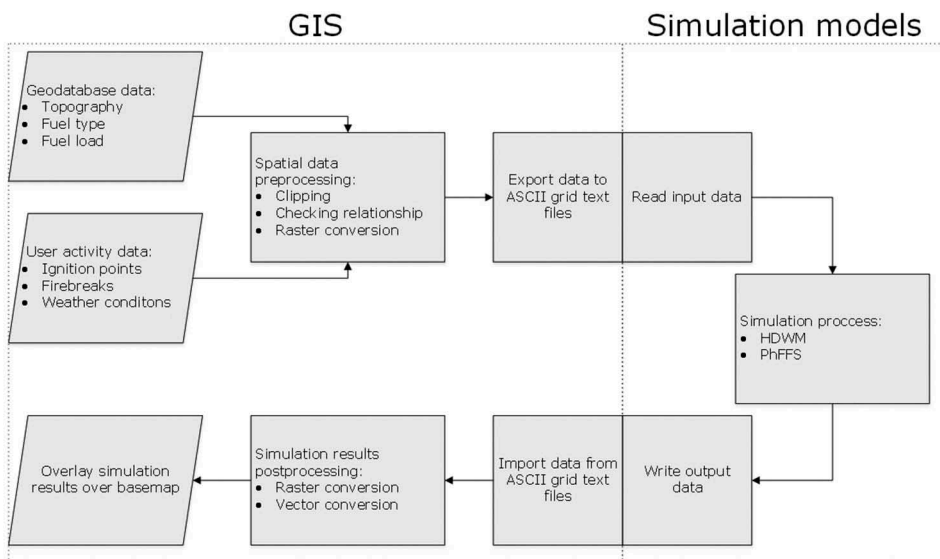

Figure 2. GIS-PhFFS-HDWM integration flow diagram.

follows (Goodchild *et al.* 1992, Nyerges 1992, Jankowski 1995, Malczewski 2006): *embedded coupling*, where there is full integration of the model within the GIS by creating user-specified routines with generic programming languages; *tight coupling*, where the model and the GIS are integrated under a common interface; and *loose coupling*, where the linkage between the GIS and the modelling system is made through the import–export of data.

The PhFFS and HDWM models have an interface provided through *ASCII grid text files* as inputs and outputs, so the easiest option for coupling these models with GIS software is a *loose coupling approach*, in which the GIS software is used to build these *ASCII grid text files* for each simulation scenario, calls the stand-alone executables of the models and reads their outputs in order to visualize them. This arrangement guarantees the same behaviour of the models both within or outside the GIS platform, reducing the amount of testing and validation required by the whole system. Adapting these models interface to GIS software involves redefining the input and output format files.

The GIS tool chosen for the integration of our models, ArcMap 10.4 of Esri's ArcGIS Desktop suite, provides options for expanding its features through custom tools. The interface with the PhFFS and HDWM models has been developed as a *Python add-in* for ArcMap. A *Python add-in* is a customization, such as a collection of tools on a toolbar, which plugs into an ArcGIS for Desktop application (ArcMap in this case) to provide supplemental functionality for performing customized tasks (ESRI 2016b).

The add-in developed includes a menu and a toolbar that contains a collection of custom tools designed to facilitate the use of the PhFFS and HDWM models. The functionality of each tool is implemented as a script using the Python programming language and the ArcPy geoprocessing library (ESRI 2016c). These scripts are run each time the user presses a button on the toolbar or on the menu, or fires a mouse event over the base map.

Following the flow diagram in Figure 2, once we have loaded the base map layer, we select the area of study and set the information over the base map to simulate a specific scenario: ignition points, wind data and eventually firebreaks, using the corresponding menu option or toolbar option or mouse event. All this information and the corresponding spatial data for the selected area are preprocessed: clipped, checked to avoid errors, converted to raster and exported to ASCII grid text files. The PhFFS and HDWM read the files they need, and the simulation is run providing the corresponding output ASCII grid text files. The post-processing step converts the output ASCII files to raster and vector files in order to display them over the base map. All the raster and vector layers used during the same simulation process are geo-referenced to the same geographical area, and have the same resolution and dimensions.

The integration of the PhFFS and HDWM models into a GIS tool achieves several objectives. First of all, it provides a simple, intuitive and easy-to-use tool that is more accessible to a broader audience that might not be familiar with PhFFS and HDWM models. Furthermore, the automation of the data acquisition and processing of all the geographical information required simplifies the simulation process reducing simulation time. It also prevents input data errors, which may cause software crashes or incorrect outputs, and ensures complete and reliable data, as well as the standardization of the geo-referenced input data. Therefore, the development of this

operational system improves its usability by a reducing simulation time and user-knowledge.

3.2. *Input spatial data*

As we described in Section 2.4, our GIS-integrated wildland fire model uses the following input data: topography, fuel load and type, weather conditions, ignition location and fire suppression tactics; and predicts the fire spread for the established time period, providing the following outputs at each time step: the burnt area perimeter and the fire front position. Likewise, our GIS-integrated wind model also uses topography, surface roughness and weather conditions, and provides a wind velocity field that is well adapted to the domain studied, defined by wind velocity.

Initially, the GIS-based wildland fire simulation tool described in this paper was developed for its use throughout Spain, so the scope of the spatial information currently used is limited to that area. We define a common spatial reference for all the heterogeneous spatial data resources. According to Spanish regulations (BOE 2007), the selected spatial reference is the Projected Coordinate System *ETRS1989 UTM Zone 30N*, except for the Canary Islands, where the Projected Coordinate System *ETRS1989 UTM Zone 28N* is used instead. All the maps and databases we mention hereafter are referred to in English with their Spanish acronym, and the corresponding copyrights are shown in the references.

The first geographical resource is the base map used to identify the area in which the simulation is to be conducted. The fire ignition point is located on the base map by a simple mouse event, as well as possible fire suppression tactics and meteorological wind data positions. Finally, this map is also used to display the simulation results. Since base maps are used in many applications, there are several options delivered as map services, ranging from public entities to private corporations, such as *ArcGIS online Base maps* (ESRI 2016a). The base map selected for our operating system is the *Spanish Topographic Base Map* provided by the © *Instituto Geográfico Nacional de España* (IGN) via a *Web Map Service* (IGN 2016).

Once the study domain has been selected, we need three raster files corresponding to the topography, fuel type and fuel load of the study domain. In order to reduce computation time, we have gathered all the necessary resources as input data, and then we have processed them to produce a geodatabase that contains the three maps needed for extracting the spatial information our models use. In this way, for each simulation it is enough to clip the data corresponding to the study domain. It is important to stress that the scope for applying the system developed can be extended to other areas by incorporating the geographical information for a new region.

The first map processed contains the height of the surface h required for both PhFFS and HDWM models. This information is provided by a *Digital Elevation Model* (DEM). We select the DEM also published by the IGN via a *Web Coverage Service* (WCS) (IGN 2013). The service offers DEMs with different resolutions – 25, 200, 500 and 1000 m – and different reference systems. The resolution selected is 25 m, with the spatial reference mentioned earlier. Since one of the requirements of a fire spread model is to provide real-time feedback, as the WCS service response time penalizes the entire system

response time, we extract the entire DEM for the whole of Spain, and store it on a geodatabase on the local hard drive.

The second map processed gathers all the information related to fuel type, provided by land cover or forestry maps. Depending on the region and/or year in which the fire to be simulated occurred, we use the *Spanish Forestry Map* 1:25,000 (MFE25) (Magrama 2016b) combined with the *Fourth Spanish National Forest Inventory* (IFN4) (Magrama 2016a) or the *Spanish Forestry Map* 1:50,000 (MFE50) (Magrama 2007a) with the information from the *Third Spanish National Forest Inventory* (IFN3) (Magrama 2007b). Both inventories have been developed by the *Ministry of Agriculture, Food and Environment* of the Spanish Government. As explained in Section 2.4, fuel type is required as an index to set the fuel type-dependent input variables for both PhFFS and HDWM models.

The third map processed collects all the elements involving the function of either artificial or natural fuelbreaks that affect the fire spread. These data have been extracted from the *Spanish Land Cover Information System* (SIOSE) (IGN 2011) by selecting all the surfaces where a fire cannot occur (barren land, waterbodies, transport infrastructures, etc.), providing zero load fuel data for the model. We should emphasize that the PhFFS model caters for fire crossing surfaces without fuel by the radiation mechanism. As mentioned earlier, the tool developed allows incorporating certain fire suppression tactics into the simulation process: the user can interactively insert firebreaks through a mouse event over the base map, adding this new information to fuel load data. It is thus possible to overcome the limitations of the static nature of the GIS to adapt the simulation to the ongoing situation. From all these data, the initial fuel load is generated.

Finally, the PhFFS model requires another last geo-referenced data, the ignition points. These points are also introduced interactively over the base map via mouse events. This information is passed to the model as the peak temperature of the solid fuel at the point where the mouse event took place, providing the initial solid fuel temperature.

Optional spatial data used by the PhFFS model involve wind velocity, which can either be computed by the HDWM model or a given value.

On the other hand, apart from the height h of the surface and the roughness length z_0, the HDWM takes the surface air temperature at each point. Such data are provided as a raster that may reflect the fire's influence on local weather conditions.

3.3. *Mapping output data*

After processing the input data provided and running the models, the simulation results are displayed on the base map. As mentioned at the end of Section 2.4, the PhFFS model provides two types of output data: the solid fuel mass fraction c and the non-dimensional solid fuel temperature u. Comparing the output solid fuel mass fraction with the initial fuel mass fraction inputted into the model provides the state of the landscape. So for each point of the domain we can determine whether or not that specific point has been burnt. This information is transformed to a vector layer and represented on the base map in order to establish the *fire perimeter* at different instants, using a layer for each time step. The solid fuel temperature is also transformed into a vector layer and

represented on the base map for identifying those areas burning at the indicated time step, establishing the *fire front position* (see Figure 6).

Likewise, the wind velocity data that the HDWM provides at different layers over the ground surface can be displayed. We represent the resulting wind field by combining this information on a feature class, and we use its attributes (module and direction) for setting the corresponding colours and arrows with the right rotation. As ArcMap can only visualize 2D scenarios, we represent the wind data corresponding to each level by using a different layer for each height level (see Figure 4).

4. Example

The tool's functionality is tested by simulating a real fire that occurred in an area near Ourense (Spain) in August 2009, comparing the simulation results with the actual fire data. The results from the simulations of this scenario indicate acceptable agreement, showing that the combination of the PhFFS model with GIS can simulate realistic wildland fire scenarios, in faster than real-time. The simulation area is a rectangle of 3.315 m × 2.740 m, and the simulation of each hour of fire spread involves about 4.30 min of computational time on a laptop equipped with an Intel i5-2410M processor (two cores, each one working at a frequency of 2.30 GHz) and 8 GB RAM. A total of 4.5 h have been simulated, reporting results every 15 min of real-time simulation and updating wind data every half hour, with a total simulation time of 20 min.

The real wildfire ignited at 3:45 pm local time on 17 August 2009 near Osoño, Ourense province, in the autonomous region of Galicia in north-western Spain, one of the country's most fire-affected areas. The firefighting team had failed to stabilize the fire by 11:00 pm on the same day, but brought it under control at 3:45 am on the following day, and finally extinguishing it at 9:10 pm on 18 August. The fire burned 224 ha: 185 ha of forest area (83 ha were tree-covered interspersed with heath) and 39 ha of agricultural area. The fire spread and its behaviour were reconstructed and documented by the coordinator of the fire-suppression operations, Morillo (2011), co-author of this paper.

The burnt area is located at an altitude ranging from 540 m (ignition point area) to 680 m (end fire area) above sea level. The average slope ranges from 6.56% at the beginning of the fire to 2.86% at the end. For the first hours, the fire spread over an uneven surface, with positive and negative discontinuous slopes, with watersheds and river basins; for the final part, although the altitude is higher, the surface is relatively flat.

Figure 3 shows the fuel data from the IFN4 with the fuel type distribution according to BEHAVE classification (Andrews 1986), adapted to Spanish forestry by the Nature Conservation Institute (MAPA 1987). The IFN4 data show some discrepancies with the observed data because the area where this fire occurred has been affected by several fires over the years, and these data are not regularly updated. This discrepancy between the available data and the actual data poses one of the challenges that fire simulation has to tackle. In this example, the initial burnt area was covered mainly with *Pinus pinaster* corresponding to model 7 (inflammable brush); the middle area was covered with model 6 (dormant brush) and to a lesser extent model 1 (short grass) and 2 (timber grass). The end burnt area was covered with diverse fuel types, mainly model 5 (brush). Basin areas and property lines were covered by thick forest, corresponding to model 9
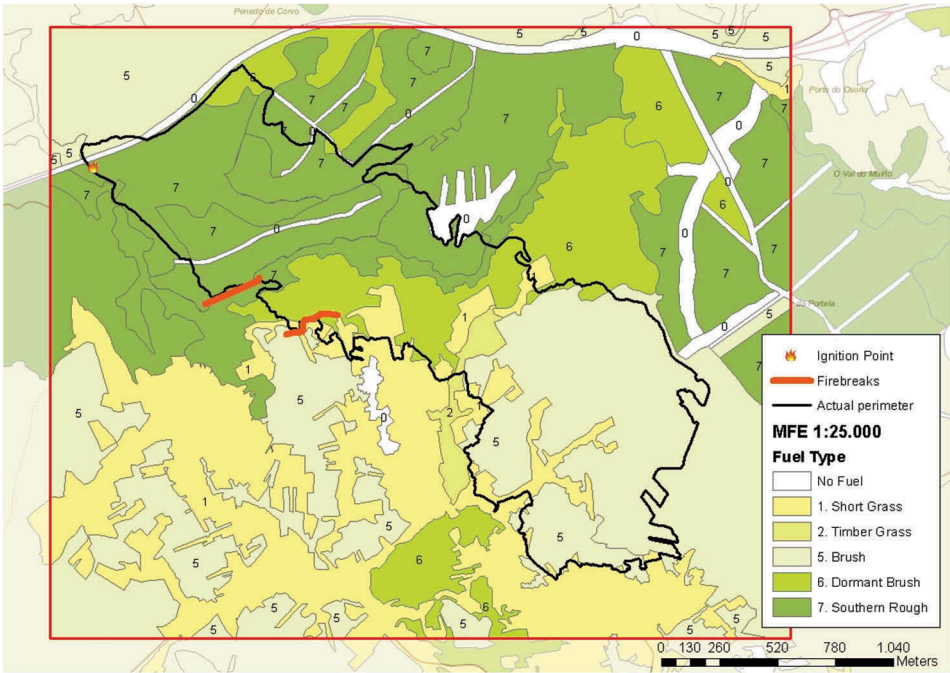
Figure 3. Simulation area (red rectangle), fire ignition point, IFN4 fuel type distribution, actual final perimeter (black line) and firefighters' firebreaks (red lines).

(dense forest) but these data do not appear in the IFN4 database. The observed data show areas with some shrubs in the middle and end areas that do not appear in the IFN4 data. Figure 3 also shows the existing fuelbreaks (20 m wide) along the crests that the actual fire crossed, as did the simulation, and two firebreaks (red lines) the firefighters made by widening two existing roads on the southern flank.

Table 3 summarizes the values of the fuel type-dependent input variables used in the example for each one of the five fuel types that appear in the IFN4 data on the studied area. These values have been identified adapting the information from Arellano *et al.* (2016) to the BEHAVE classification for the PhFFS model fuel type-dependent input variables. The values for the roughness length z_0 used for the HDWM are taken from Wieringa (1992).

Weather data (wind, temperature and relative humidity) were collected every 10 min at a nearby weather station (3750 m away) at a height of 10 m and were incorporated into the simulation process every 30 min. Table 4 summarizes the average hourly

Table 3. Used values for fuel type-dependent input variables.

Fuel type	Description	M_0 (kg m^{-2})	M_v	T_f (K)	T_p (K)	$t_{1/2}$ (s)	F (m)	C (J K^{-1} kg^{-1})	z_0 (m)
1	Short grass	0.1	0%	1300	500	100	2.5	1800	0.08
2	Timber grass	1.0	10%	1300	500	100	4	2000	0.08
5	Brush	2.3	10%	1300	500	200	5.5	2300	0.1
6	Dormant brush	2.2	10%	1300	500	200	7	2300	0.1
7	Inflammable brush	2.4	15%	1300	500	200	8	2300	0.1

Table 4. Meteorological data.

Local time	Temperature (°C)	Humidity (%)	Wind speed (m s^{-1})	Wind direction°	Wind gust (m s^{-1})
3:45–5:00 pm average	32.02	27.17	3.18	319.39	5.62
5:00–6:00 pm average	32.01	27.43	4.79	341.29	7.76
6:00–7:00 pm average	31.50	27.43	4.42	334.00	7.44
7:00–8:00 pm average	31.42	27.50	4.48	335.00	7.45
8:00–9:00 pm average	30.11	30.00	4.42	344.33	7.24
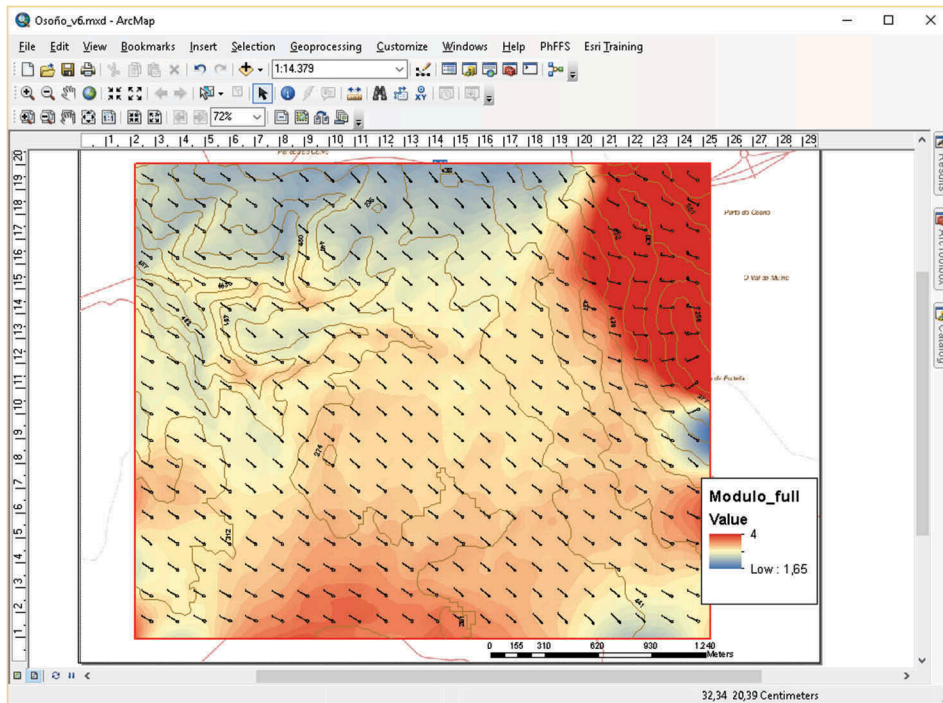
Figure 4. Screenshot of the GIS interface displaying the wind field simulated with HDWM at 7 pm, at a height of 10 m, along the simulation area.

ambient temperature (Celsius), relative air humidity (%), wind speed (m s^{-1}) and direction (degree from North), and wind gust (m s^{-1}). Figure 4 shows the wind field simulated with the HDWM at a height of 10 m, corresponding to meteorological data at 7 pm.

The coupling effect of wind and topography considerably influenced this fire spread rate and direction. Initially, wind velocity was moderate, about 3.18 m s^{-1} from the west. As the afternoon progressed, the wind velocity increased to 4.79 m s^{-1} with gusts of almost 8 m s^{-1}, and turning slightly to the north. This caused secondary fire sources due to the transport of firebrands by convection columns. Most of the firefighters' actions by land and air over the fire flanks are not reflected in the simulation, nor are the secondary fire sources, due to insufficient information, except those firebreaks made by widening some existing roads, where the available information is sufficiently detailed. Despite that, the simulated and actual perimeters are quite similar, as shown in Figure 5, where the actual and simulated perimeters at 5, 6, 7 and 8 pm are outlined together
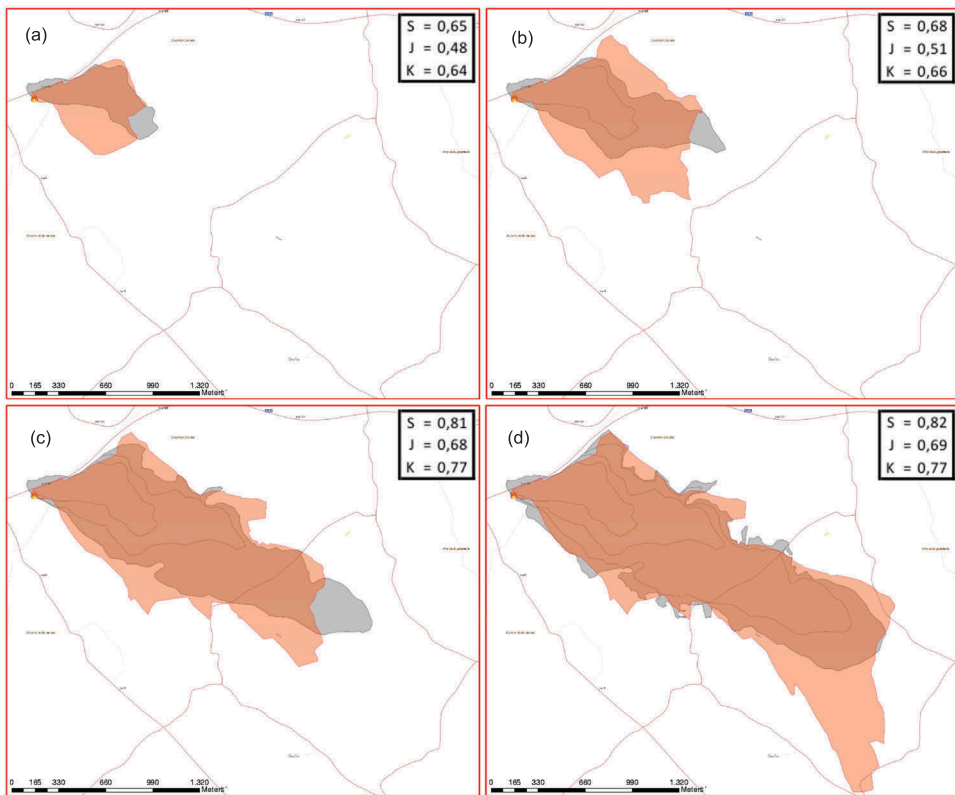
Figure 5. Comparison of the actual (grey) and simulated (orange) perimeter at 5 pm (a), 6 pm (b), 7 pm (c) and 8 pm (d), and the corresponding Sørensen similarity index (S), Jaccard similarity coefficient (J), and Kappa coefficient (K).

with the corresponding Sørensen similarity index (S), Jaccard similarity coefficient (J) and Kappa coefficient (K) (Filippi *et al*. 2014). These coefficients range from 1 and 1; 1 means a perfect agreement between observation and simulation, and 0 means there is no agreement. The average values obtained, $\bar{S} = 0.74$, $\bar{J} = 0.59$ and $\bar{K} = 0.71$, show *substantial agreement* (Filippi *et al*. 2014). The largest differences between the actual and simulated perimeters arises in the latest instant due to the increased fire-fighters' actions not reflected in the simulation (see Figure 5(d)).

Figure 6 shows the actual perimeter (black line) and simulated fire at 7 pm in the GIS interface. The simulated fire differentiates between active fire front (orange) and burnt area (grey).

5. Conclusions

This paper presents a GIS-based interface for two simplified physical models, a wildland fire spread model, PhFFS, and a wind field model, HDWM, which can work coupled or separately. The development of this tool is based on the extent of the functionality of the GIS commercial software ArcGIS, through the Python scripting language and Esri's ArcPy library. Several scripts have been developed to automate geographical data
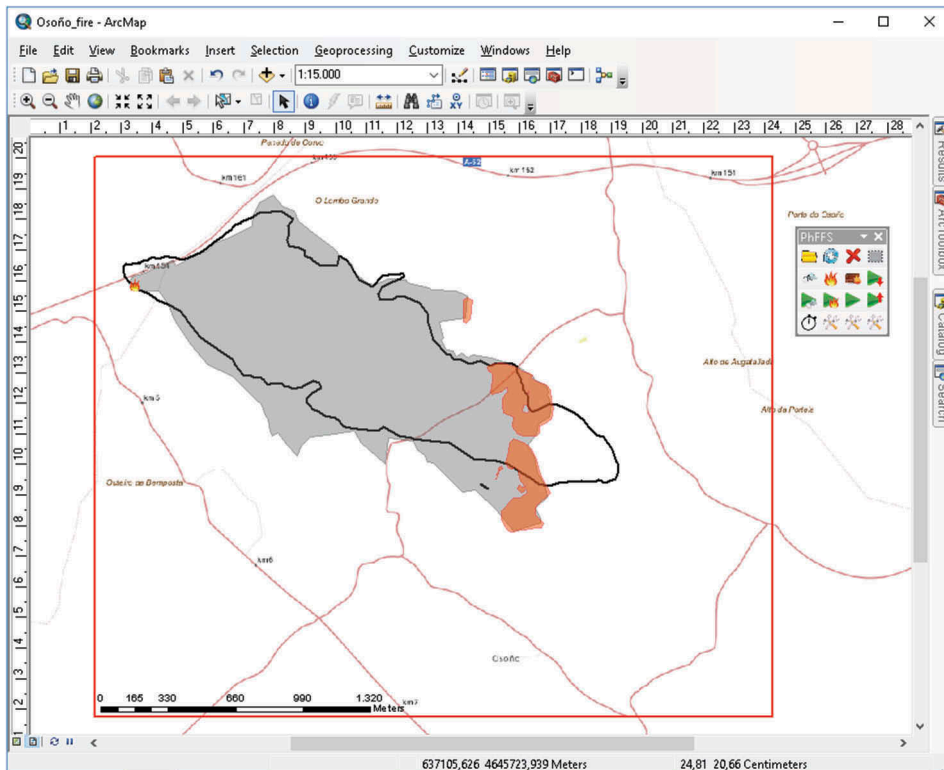
Figure 6. Screenshot of the GIS interface displaying the actual perimeter (black line) and simulated fire: burnt area (grey) and active fire front (orange) after 3.15 h of fire ignition (7 pm).

acquisition, spatial data preprocessing, model running and the visualization of the simulation results on a base map.

The initial purpose of the integration of the fire and wind models on a GIS-based interface is to facilitate the testing and validation process, by automating and simplifying the data acquisition process and the display of the solution.

The GIS-based tool achieves a second purpose, as it makes the PhFFS and HDWM models more readily accessible to the potential end-user by providing a simple, intuitive and easy-to-use tool that is more accessible to a broader audience that might not be familiar with these models.

The complete simulation of either one of the physical processes that the tool supports, wildland fire spread or wind field, includes three steps: preprocessing the requested data, calculating the models and post-processing the solution. The scripts developed reduce preprocessing and post-processing times and prevent input data errors. The numerical techniques that both PhFFS and HDWM use guarantee shorter-than-real-time computational times. Reducing the total computational time is critical for the practical application of these models.

Some direct applications of the PhFFS model are the design of risk mapping, reforestation policies or fuelbreaks in prevention operations; the optimization of firefighting resources, risk prevention, the issue of warnings or evacuation planning in suppression operations, along with others such as prescribed burn planning.

Certain additional functionalities of the designed tool may have an interesting potential for practical applications. Secondary fire sources (spotting) can be simulated by adding new ignition points. Some suppression works, such as firebreaks, can be simulated through the 'firebreaks tool' on the application toolbar, enabling the user to test different scenarios.

The HDWM has other specific applications, such as wind power forecasting on wind farms.

Finally, the real analysed wildland fire pointed out the utility of the system through a realistic simulation of the wildfire spread, showing a substantial agreement between simulation and observation.

Note

1. ArcGIS® and ArcMap™ are the intellectual property of Esri and are used herein under license. Copyright© Esri. All rights reserved. For more information about Esri® software, please visit www.esri.com.

Acknowledgements

Disclosure statement

No potential conflict of interest was reported by the authors.

Funding

ORCID

D. Prieto Herráez ⬤ http://orcid.org/0000-0003-4636-2261
M. I. Asensio Sevilla ⬤ http://orcid.org/0000-0002-8713-5594
L. Ferragut Canals ⬤ http://orcid.org/0000-0001-5730-4281
J. M. Cascón Barbero ⬤ http://orcid.org/0000-0003-3650-6188
A. Morillo Rodríguez ⬤ http://orcid.org/0000-0002-1461-0593

References

Ager, A.A., Vaillant, N.M., and Finney, M.A., 2011. Integrating fire behavior models and geospatial analysis for wildland fire risk assessment and fuel management planning. *Journal of Combustion*, 2011, 1–19. doi:10.1155/2011/572452

Anderson, H.E., 1982. *Aids to determining fuel models for estimating fire behavior*. Ogden, UT: U.S. Department of Agriculture, Forest Service, Intermountain Forest and Range Experiment Station, General Technical Report INT-122.

Anderson, H.E., 1969. *Heat transfer and Forest Fire*. Ogden, UT: U.S. Department of Agriculture, Forest Service, Intermountain Forest and Range Experiment Station, General Technical Report INT-69.

Andrews, P., 1986. *Behave: fire behaviour prediction and fuel modellings system - burn subsystem, part 1*. Ogden, UT: U.S. Department of Agriculture, Forest Service, Intermountain Forest and Range Experiment Station, General Technical Report INT-194.

Arellano, S., *et al.* 2016. *Foto-Guía de combustibles forestales de Galicia*. Santiago de Compostela: Andavira Editora, S.L.

Asensio, M. and Ferragut, L., 2002, On a wildland fire model with radiation. *International Journal for Numerical Methods in Engineering*, 54 (1), 137–157. doi:10.1002/(ISSN)1097-0207

Asensio, M., Ferragut, L., and Simon, J., 2002, Modelling of convective phenomena in forest fire. *RACSAM - Revista de la Real Academia de Ciencias Exactas, Físicas y Naturales. Serie A. Matemáticas*, 96 (3), 299–313.

Asensio, M., Ferragut, L., and Simon, J., 2005. A convection model for fire spread simulation. *Applied Mathematics Letters*, 18 (6), 673–677. Special issue on the occasion of MEGA 2003. doi:10.1016/j.aml.2004.04.011

BOE, 2007. Real Decreto 1071/2007, de 27 de julio, por el que se regula el sistema geodésico de referencia oficial en España. *Boletín Oficial del Estado* [online]. Available from: http://www.fomento.gob.es/NR/rdonlyres/5B614FA3-5B57-4838-9D08-1434B8FD2DD5/70540/RD10712007.pdf [in Spanish] [Accessed May 2016]. 335915062293500

Cascón, J., *et al.*, 2016. A reduced basis for a local high definition wind model. *Computer Methods in Applied Mechanics and Engineering*, 311, 438–456. doi:10.1016/j.cma.2016.08.028

Chapman, B., Jost, G., and Pas, R.V.D., 2008. *Using OpenMP: portable shared memory parallel programming*. Cambridge, Mass: Scientific and Engineering Computation MIT Press.

Chuvieco, E. and Duarte, L., 1996, Mapping the spatial distribution of forest fire danger using GIS. *International Journal of Geographical Information Science*, 10 (3), 333–345. doi:10.1080/02693799608902082

Coleman, J. and Sullivan, A., 1996. A real-time computer application for the prediction of fire spread across the Australian landscape. *Simulation*, 67, 230–240. doi:10.1177/003754979606700402

Davenport, A., *et al*. 2000. Estimating the roughness of cities and sheltered country. *In*: *Preprints Twelfth Conference on Applied Climatology*, Asheville, NC: United States American Meteorological Society, 96–99.

ESRI, 2016a. ArcGIS online basemaps. [online]. Available from: http://www.esri.com/data/basemaps [Accessed May 2016a].

ESRI, 2016b. What is a Python add-in? *Help documents collection from ArcGIS Online* [online]. Available from: http://desktop.arcgis.com/en/arcmap/10.3/guide-books/python-addins/what-is-a-python-add-in.htm [Accessed May 2016b].

ESRI, 2016c. What is ArcPy? *Help documents collection from ArcGIS Online* [online] Available from: https://desktop.arcgis.com/en/arcmap/10.3/analyze/arcpy/what-is-arcpy-.htm [Accessed May 2016c].

FAO, 2007. *Fire-management global assessment 2006. A thematic study in the framework of the Global Forest Resources Assessment 2005*. Technical report FAO Forestry Paper 151, Food and Agriculture Organization of the United Nations, Rome.

Ferragut, L., *et al*. 2014. No. 4 SEMA SIMAI Springer series, A simplified wildland fire model applied to a real case. *In*: *Advances in differential equations and applications*, Cham: Springer International Publishing, 155–167.

Ferragut, L., *et al*. 2015. A wildland fire physical model well suited to data assimilation. *Pure and Applied Geophysics*, 172 (1), 121–139. doi:10.1007/s00024-014-0893-9

Ferragut, L., Asensio, M., and Monedero, S., 2007a, Modelling radiation and moisture content in fire spread. *Communications in Numerical Methods in Engineering*, 23 (9), 819–833. doi:10.1002/cnm.927

Ferragut, L., Asensio, M., and Monedero, S., 2007b, A numerical method for solving convection-reaction-diffusion multivalued equations in fire spread modelling. *Advances in Engineering Software*, 38 (6), 366–371. doi:10.1016/j.advengsoft.2006.09.007

Ferragut, L., Asensio, M., and Simon, J., 2011, High definition local adjustment model of 3D wind fields performing only 2D computations. *International Journal for Numerical Methods in Biomedical Engineering*, 27 (4), 510–523. doi:10.1002/cnm.v27.4

Filippi, J., Mallet, V., and Nader, B., 2014. Representation and evaluation of wildfire propagation simulations. *International Journal of Wildland Fire*, 23, 46–57. doi:10.1071/WF12202

Finney, M., 2004. *FARSITE: fire Area Simulatormodel development and evaluation*. Research Paper RMRS-RP-4 (revised), U.S. Department of Agriculture, Forest Service, Rocky Mountain Research Station, Ogden, UT.

Finney, M., *et al.* 2015. Role of buoyant flame dynamics in wildfire spread. *Proceedings of the National Academy of Sciences of the United States of America*, 112 (32), 9833–9838. doi:10.1073/pnas.1504498112

Flannigan, M.D., *et al.* 2009. Implications of changing climate for global wildland fire. *International Journal of Wildland Fire*, 18 (5), 483–507. doi:10.1071/WF08187

Frankman, D., *et al.* 2013. Measurements of convective and radiative heating in wildland fires. *International Journal of Wildland Fire*, 22 (2), 157–167. doi:10.1071/WF11097

Goodchild, M., *et al.* 1992. Integrating GIS and spatial data analysis: problems and possibilities. *International Journal of Geographical Information Systems*, 6 (5), 407–423. doi:10.1080/02693799208901923

Gopalan, H., *et al.*, 2014. A coupled mesoscale-microscale framework for wind resource estimation and farm aerodynamics. *Journal of Wind Engineering and Industrial Aerodynamics*, 132, 13–26. doi:10.1016/j.jweia.2014.06.001

Hilton, J., *et al.*, 2015. Effects of spatial and temporal variation in environmental conditions on simulation of wildfire spread. *Environmental Modelling & Software*, 67, 118–127. doi:10.1016/j.envsoft.2015.01.015

IGN, 2011. Spanish Land Cover Information System. *Instituto Geográfico Nacional de España* [online]. Available from: http://www.ign.es/ign/layoutIn/siose.do [Accessed May 2016].

IGN, 2013. Spanish Digital Elevation Model. *Instituto Geográfico Nacional de España* [online]. Available from: http://www.ign.es/wcs/mdt [Accessed May 2016].

IGN, 2016. IGN Spanish Base Map. *Instituto Geográfico Nacional de España* [online]. Available from: http://www.ign.es/wms-inspire/ign-base [Accessed May 2016].

Jankowski, P., 1995, Integrating geographical information systems and multiple criteria decision-making methods. *International Journal of Geographical Information Systems*, 9 (3), 251–273. doi:10.1080/02693799508902036

Linn, R., *et al.* 2002. Studying wildfire behavior using FIRETEC. *International Journal of Wildland Fire*, 11 (4), 233–246. doi:10.1071/WF02007

Linn, R.R., 1997. *A transport model for prediction of wildfire behavior*. NM: Los Alamos National Lab, Technical report LA-13334T.

Lopes, A., Cruz, M., and Viegas, D., 2002, FireStation - an integrated software system for the numerical simulation of fire spread on complex topography. *Environmental Modelling & Software*, 17 (3), 269–285. doi:10.1016/S1364-8152(01)00072-X

Magrama, 2007a. Spanish Forestry Map 1:50,000. *Ministerio de Agricultura, Alimentación y Medio Ambiente* [Online], 3 (4). Available from: http://www.magrama.gob.es/es/biodiversidad/servicios/banco-datos-naturaleza/informacion-disponible/mfe50.aspx [[Retrieved: May 2016a]].

Magrama, 2007b. Third Spanish National Forest Inventory. *Ministerio de Agricultura, Alimentación y Medio Ambiente* [Online]. Available from: http://www.magrama.gob.es/es/biodiversidad/servicios/banco-datos-naturaleza/informacion-disponible/ifn3.aspx [[Retrieved: May 2016b]].

Magrama, 2016a. Fourth Spanish National Forest Inventory. *Ministerio de Agricultura, Alimentación y Medio Ambiente* [Online]. Available from: http://www.magrama.gob.es/es/desarrollo-rural/temas/politica-forestal/inventario-cartografia/inventario-forestal-nacional/ [[Retrieved: May 2016a]].

Magrama, 2016b. Spanish Forestry Map 1:25,000. *Ministerio de Agricultura, Alimentación y Medio Ambiente* [Online]. Available from: http://www.magrama.gob.es/es/desarrollo-rural/temas/politica-forestal/inventario-cartografia/mapa-forestal-espana/mfe25.aspx   [[Retrieved: May 2016b]].

Malczewski, J., 2006, GIS-based multicriteria decision analysis: a survey of the literature. *International Journal of Geographical Information Science*, 20 (7), 703–726. doi:10.1080/13658810600661508

Mandel, J., *et al.*, 2014. Recent advances and applications of WRF-SFIRE. *Natural Hazards and Earth System Sciences*, 14, 2829–2845. doi:10.5194/nhess-14-2829-2014

Mandel, J., Beezley, J.D., and Kochanski, A.K., 2011, Coupled atmosphere-wildland fire modeling with WRF 3.3 and SFIRE 2011. *Geoscientific Model Development*, 4 (3), 591–610. doi:10.5194/gmd-4-591-2011

MAPA, 1987. *Photographic key to the identification of fuel models*. Madrid: Ministerio de Agricultura Pesca y Alimentación, Instituto para la Conservación de la Naturaleza ICONA, Technical report. [in Spanish].

Morillo, A., 2011. *Análisis del comportamiento del fuego forestal observado y simulado: estudio del caso del incendio forestal de Osoño (Vilardevós)-Verín-Ourense*. Spain: Master of advances studies work, Higher Politechnical School of Lugo, University of Santiago de Compostela. (in Spanish).

Nyerges, T., 1992. Coupling GIS and spatial analytical models. In: P. Bresnahan, Cowen, D., eds. *Proceedings of fifth International Symposium on Spatial Data Handling*. 3–7 July 1992, Charleston, SC: Humanities and Social Sciences Computing Laboratory, University of South Carolina. 534–543.

Pastor, E., *et al.* 2003. Mathematical models and calculation systems for the study of wildland fire behaviour. *Progress in Energy and Combustion Science*, 29 (2), 139–153. doi:10.1016/S0360-1285(03)00017-0

Perry, G., Sparrow, A., and Owens, I., 1999, A GIS-supported model for the simulation of the spatial structure of wildland fire, Cass Basin, New Zealand. *Journal of Applied Ecology*, 36 (4), 502–518. doi:10.1046/j.1365-2664.1999.00416.x

Prieto, D., *et al.*, 2015. Sensitivity analysis and parameter adjustment in a simplified physical wildland fire model. *Advances in Engineering Software*, 90, 98–106. doi:10.1016/j.advengsoft.2015.08.001

Reisner, J., Bossert, J., and Winterkamp, J., 1997. *Numerical simulations of two wildfire events using a combined modeling system (HIGRAD/BEHAVE)*. NM: Los Alamos National Lab, Technical report LA-UR-97-4036.

Rothermel, P., 1972. *A mathematical model for predicting fire spread in wildland fuels*. Research Paper INT-115, U.S. Department of Agriculture, Forest Service.

Scott, J. and Burgan, R., 2005. *Standard fire behavior fuel models: a comprehensive set for use with rothermel's surface fire spread model*. Fort Collins, CO: U.S. Department of Agriculture, Forest Service, Rocky Mountain Research Station, General Technical Report RMRS-GTR-153.

Skidmore, A., 2002. *Environmental modelling with GIS and remote sensing*. London: Taylor & Francis.

Sullivan, A., 2009a, Wildland surface fire spread modelling, 1990-2007. 1: physical and quasi-physical models. *International Journal of Wildland Fire*, 18 (4), 349–368. doi:10.1071/WF06143

Sullivan, A., 2009b, Wildland surface fire spread modelling, 1990-2007. 2: empirical and quasi-empirical models. *International Journal of Wildland Fire*, 18 (4), 369–386. doi:10.1071/WF06142

Tymstra, C., *et al.*, 2010. *Development and structure of Prometheus: the Canadian wildland fire growth simulation model*. Edmonton, Alberta: Canadian Forest Service, Northern Forestry Centre, Information Report NOR-X-417.

Vasconcelos, M. and Guertin, D., 1992, FIREMAP - simulation of fire growth with a geographic information system. *International Journal of Wildland Fire*, 2 (2), 87–96. doi:10.1071/WF9920087

Viegas, D., 2004, Slope and wind effects on fire propagation. *International Journal of Wildland Fire*, 13 (2), 143–156. doi:10.1071/WF03046

Wieringa, J., 1992, Updating the Davenport roughness classification. *Journal of Wind Engineering and Industrial Aerodynamics*, 41 (1–3), 357–368. doi:10.1016/0167-6105(92)90434-C

Williams, T.M., Williams, B.J., and Song, B., 2014. Modeling a historic forest fire using GIS and FARSITE. *Mathematical & Computational Forestry & Natural Resource Sciences*, 6 (2), 80–88.

Yassemi, S., Dragićević, S., and Schmidt, M., 2008, Design and implementation of an integrated GIS-based cellular automata model to characterize forest fire behaviour. *Ecological Modelling*, 210 (1–2), 71–84. doi:10.1016/j.ecolmodel.2007.07.020